Comparison of manganese oxide nanoparticles and manganese sulfate with regard to oxidative stress, uptake and apoptosis in alveolar epithelial cells

Frick, R A

Supplementary information

Protocol S1:

Nanoparticle preparation

Nanoparticles were prepared by flame spray synthesis using the metals manganese, titanium and cerium dissolved in 2-ethylhexanoic acid as precursors (Athanassiou et al., 2010; Madler et al., 2002). A detailed description of the flame spray process and set-up is given by Loher et al. (2005). Nanoparticles were dry-heat sterilized for 3 hours at 160°C and dispersed in distilled water. Stock dispersions of 200 parts per million (ppm, corresponds to µg particles per ml cell culture medium; further referred to as ppm) were sonicated for 10 min using a B-15 Branson Sonifier (pulsed, output 6.0; duty cycle 60%) to break up agglomerates and diluted to final exposure concentrations in assay medium prior to application.

Nanoparticle characterization

The Brunauer-Emmett-Teller (BET) method was used to measure the specific surface area (SSA) of the nanoparticles. Samples were outgassed at 150 °C for one hour prior to analysis and subsequently measured on a Tristar (Micromeritics Instruments) instrument by nitrogen adsorption at 77 K. The average BET-equivalent particle diameter dBET was calculated using $dBET = 6/(SSA \cdot \rho)$, where ρ denotes the density (kg m^{-3}), assuming monodisperse particles. X-ray disc centrifugation (XDC, Brookhaven Instruments, instrumental cutoff below 5 nm) was used to measure full particle size analyses. Prior to measurements particles were dispersed in ultrapure water (Millipore, resistivity > 18 MΩ cm^{-1}) and stabilized with Dispex A40 (Ciba Specialty Chemicals). After 5 minutes of sonication (Hielscher UP- 400S) the hydrodynamic particle diameter was measured on an X-ray disc centrifuge. X-ray powder diffraction (XRD) patterns were collected on a Bruker D 8 Advance diffractometer from 15° to 50° at a step size of 0.12° and a scan speed of 2.4° min^{-1} at ambient condition to confirm identity and crystallinity of materials (Stark, 2011). For the analysis of particle shape, suspensions were pipetted onto coated Transmission Electron Microscopy (TEM) grids and dried at room temperature. The samples were investigated by a Morgagni TEM (FEI, Eindhoven, The Netherlands), operated at 80 kV and equipped with a Morada camera (Gloor Instruments AG, Uster, Switzerland).

Protocol S2:

Determination of total and oxidized Glutathione:

After exposure to NPs, 250 µl of cell supernatants were collected and acidified with 2.5 µl HCl 1 M. 10 µl of the acidified supernatants were taken off for analysis of the total protein content. After precipitation of proteins by adding 32.5 µl 5-Sulfosalicylic acid 6.5% (w/v) (SSA) and centrifugation, supernatants were stored at -80°C until the assay. Cells were washed twice with 300 µl HBSS per well and subsequently lysed by adding 150 µl HCl 10 mM and freezing at -80°C. Afterwards, cells were thawed while being shaken on a plate reader for ten minutes. Cells were removed with a cell scraper, transferred to pre-chilled 1.5 ml Eppendorf tubes and sonicated in icy water for three minutes. After vortexing the tubes, 10 µl of the cell homogenates were taken off for the protein assay prior to deproteinization by adding SSA and centrifugation. Cell homogenates were stored at -80°C until the assay.

Before starting the enzymatic recycling assay, 2 µl 2-vinylpyridine was added to an aliquot of 100 µl of every sample (to the aliquot of the cell lysates as well as to the aliquot of the cell supernatant), standard and blank in order to derivatize reduced Glutathione (GSH). The remaining reagents were diluted and processed in 96-well assay plates as described by Vandeputte et al. (1994).

After addition of glutathione reductase to start the reaction, the 96-well assay plate was shaken 15 seconds and immediately absorbance was read kinetically over 5 minutes at 405 nm, at 30 seconds intervals. The rate of changes in absorbance was calculated over the linear portion of the reaction for each standard, blank and sample. Glutathione concentrations in the samples were determined by using linear regression to calculate the values obtained from the standard curve. Glutathione concentrations were expressed as nmol mg^{-1} protein.

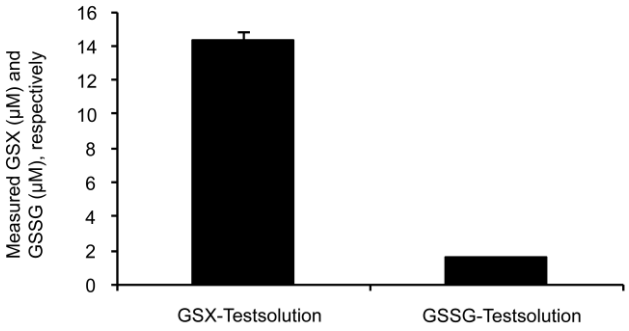

Figure S1: In order to establish and adjust the glutathione assay, pretests were run, comparing expected and measured values. The figure shows the measured values for total (GSX) and oxidized glutathione (GSSG) in a test solution. To prepare the test solution, a 20 µM stock of reduced glutathione (GSH) was mixed with a 3 µM stock of oxidized glutathione (GSSG) in the ratio of 1:2. Final concentrations of GSH and GSSG thus, were 10 µM GSH and 1.5 µM GSSG. After addition of the GSH-scavenger 2-vinylpyridine, the remaining amount of GSSG was expected to be around 1.5 µM (GSSG-Testsolution). Without the scavenger (GSX-Testsolution), total glutathione (GSX) was expected to be around 13 µM (10 µM GSH + 2 x 1.5 µM GSSG). Values of the pretests showed a slight overestimation of both, GSSG and GSX.

	Mn_3O_4-NPs	TiO_2-NPs	CeO_2-NPs
SSA [m^2/g]	39	48	32
d_{BET} [nm]	31.7	29.5	24.5

Table S1: The surface-equivalent primary particle diameter (dBET), assuming spherical, monodispersed particles, was calculated to be within the range of 30 nm. Calculation was performed using $dBET = 6/(SSA \cdot \rho)$. (ρ: density (kg m^{-3}), SSA: specific surface area (m^2/g)).

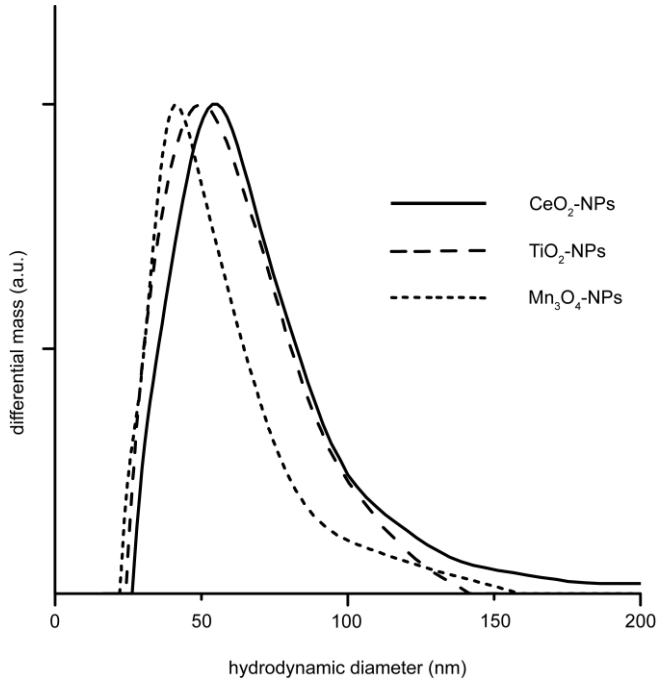

Figure S2: The size distribution of the particles was measured by X-Ray Disc Centrifuge. In suspension, the mean agglomerate size (dhydr) was around 100 nm and confirmed the presence of small agglomerates as typically found in such technically used engineered nanoparticles (Brunner et al., 2006; Limbach et al., 2005).

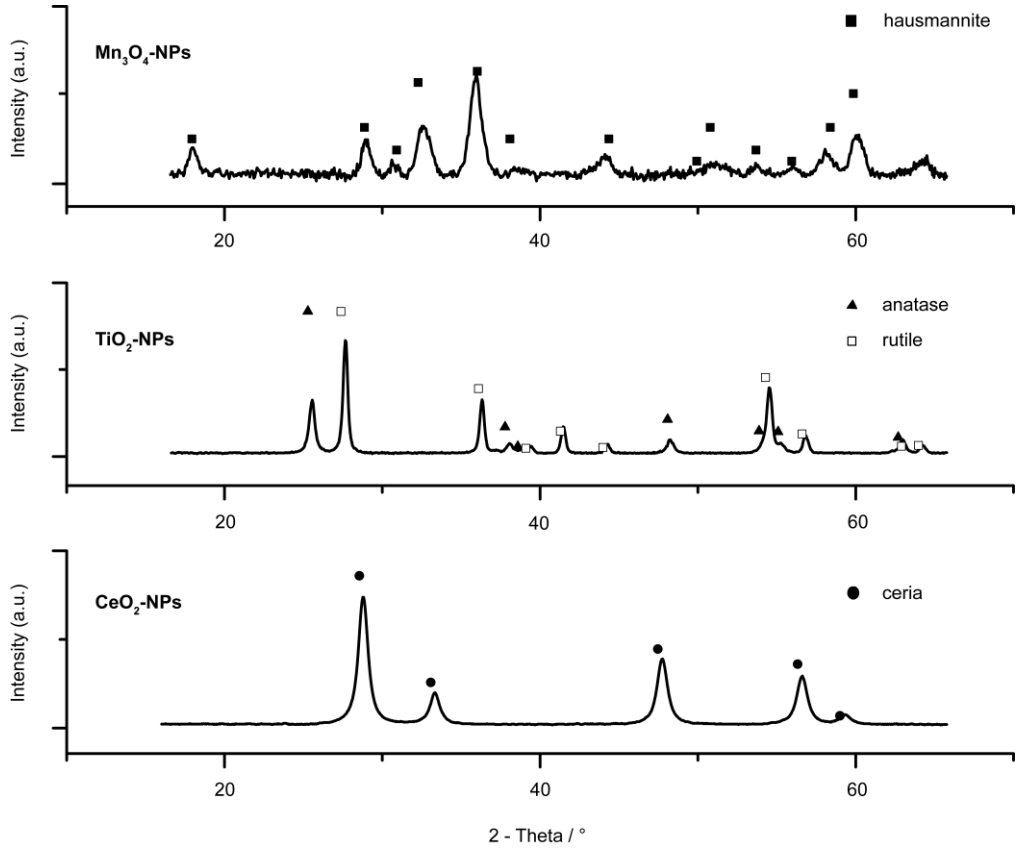

Figure S3: X-ray powder diffraction (XRD) patterns of the metal oxide nanoparticles. Manganese oxide nanoparticles (Mn_3O_4-NPs) were in the hausmannite phase and titanium dioxide nanoparticles (TiO_2-NPs) consisted of a mixture of anatase and rutile. Identity of cerium dioxide nanoparticles was confirmed.

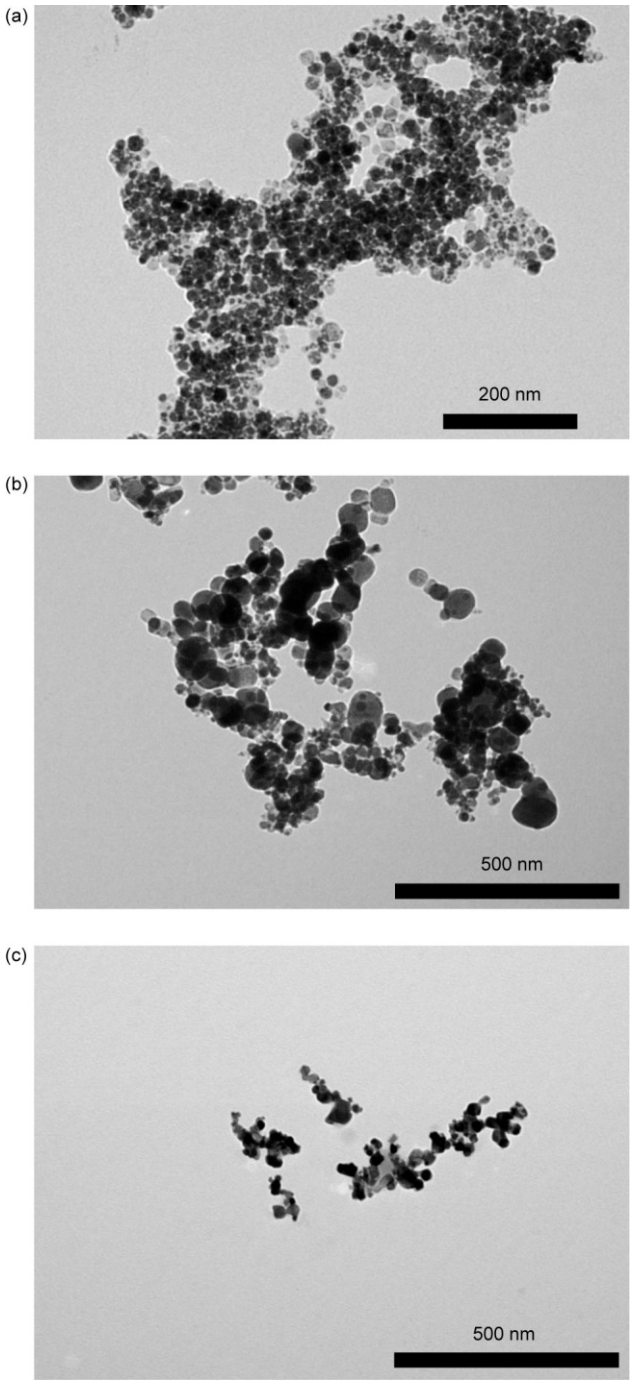

Figure S4: TEM images of aqueous suspensions of (a) Mn_3O_4-NPs, (b) TiO_2-NPs and (c) CeO_2-NPs. Manganese oxide- and titanium dioxide nanoparticles were spherical, whereas cerium dioxide nanoparticles appeared as sharp edged, cubic crystals.

	control	sin-1	TiO_2-NPs	CeO_2-NPs
ROS (% of control)	100	207	133	110
SD	16,7	35,7	36,7	15,7

Table S2: Quantification of reactive oxygen species (ROS) generation in cells exposed to TiO_2-NPs (20 ppm) and CeO_2-NPs (20 ppm) for 24 hours. Experiments were performed as described by Limbach et al. (2007). SIN-1 (3-morpholino-sydnonimine hydrochloride) was used as positive control. Experiments were carried out in triplicates and repeated three times. Values are mean ± SD.

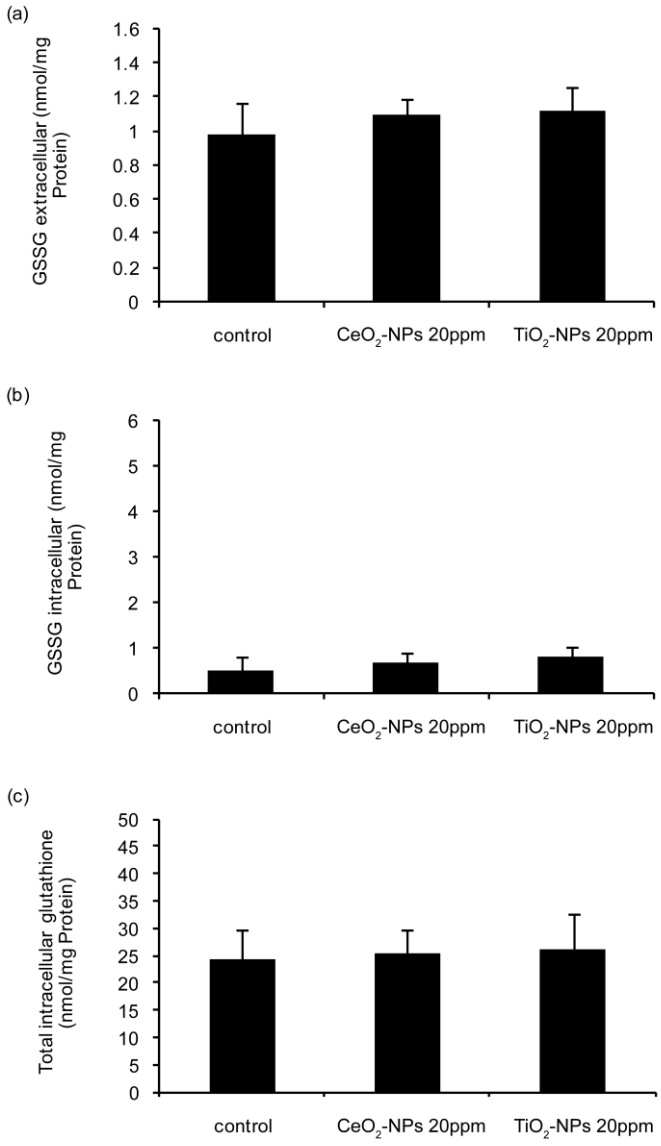

Figure S5: Concentration of oxidized glutathione (GSSG) and total intracellular glutathione in cells exposed to TiO_2-NPs and CeO_2-NPs for 24 hours. Cells were incubated with 20 ppm TiO_2-NPs and CeO_2-NPs for 24 hours. GSSG was determined in the supernatant (a) and within alveolar epithelial cells (b). In addition total intracellular glutathione (reduced and oxidized) was measured (c). Experiments were carried out in triplicates and repeated at least twice. Values are mean ± SD. No significant changes in glutathione contents could be detected.

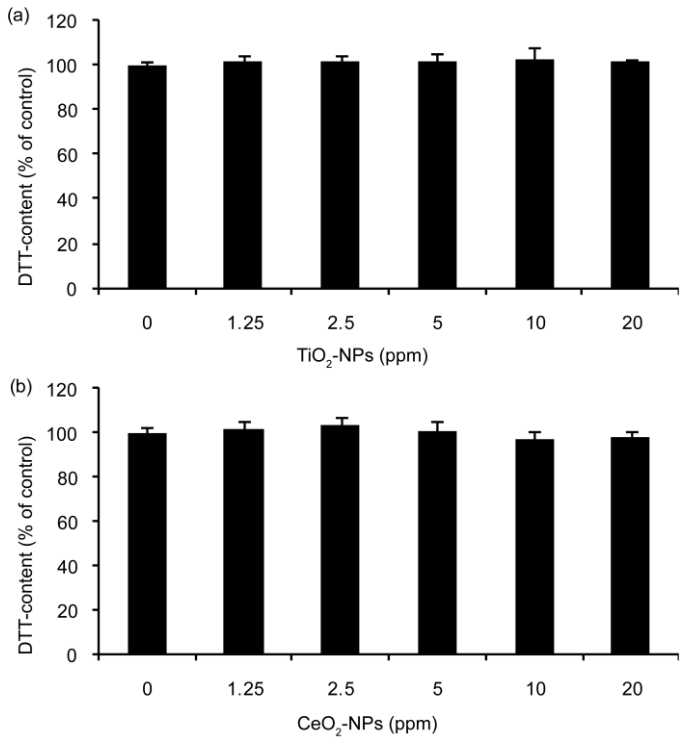

Figure S6: Effect of (a) titanium dioxide nanoparticles (TiO_2-NPs) and (b) cerium dioxide nanoparticles (CeO_2-NPs) on dithiothreitol (DTT) contents in an abiotic environment after one hour of incubation. Experiments were carried out in triplicates and repeated at least twice. Values are mean ± SD. No significant changes in DTT contents could be detected.

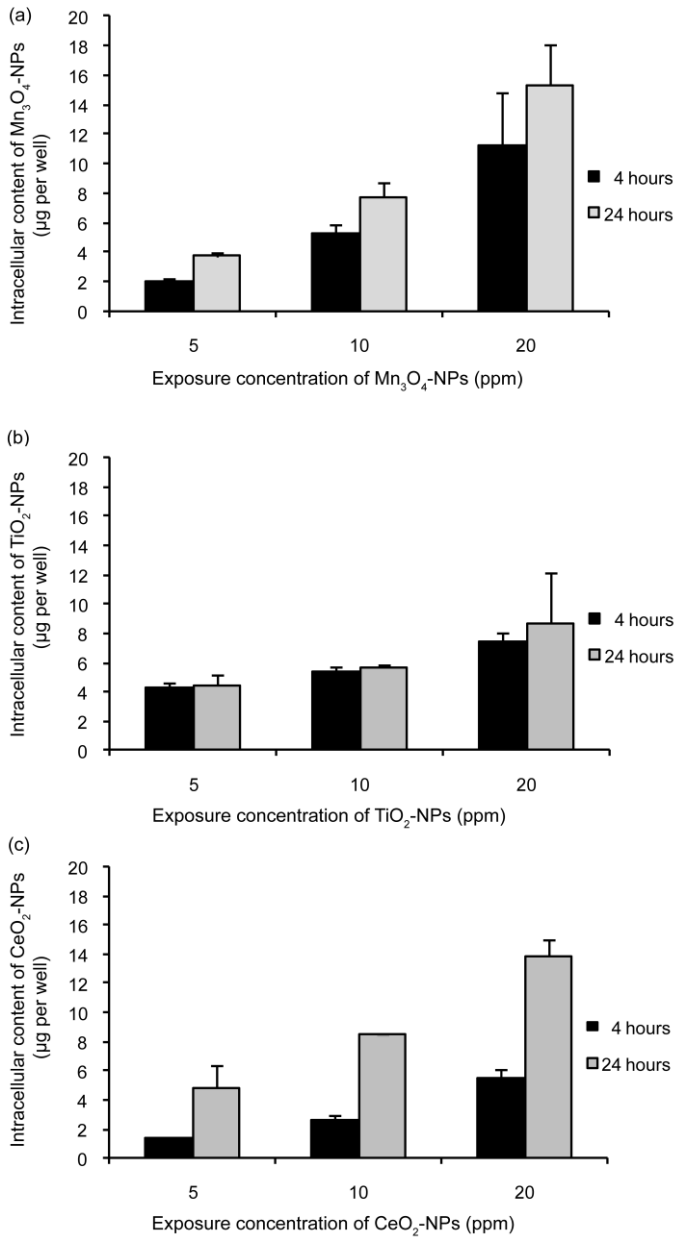

Figure S7. Intracellular contents of nanoparticles determined by inductively coupled plasma mass spectrometer. Values were calculated from the intracellular contents of transition metal per well. Cells were exposed to (a) manganese(II,III) oxide nanoparticles (Mn_3O_4-NPs), (b) titanium dioxide nanoparticles (TiO_2-NPs) and (c) cerium dioxide nanoparticles (CeO_2-NPs) for 4 (black bars) and 24 hours (grey bars). Values represent the average intracellular contents of NPs per well. Values are mean ± SD of two to four wells.

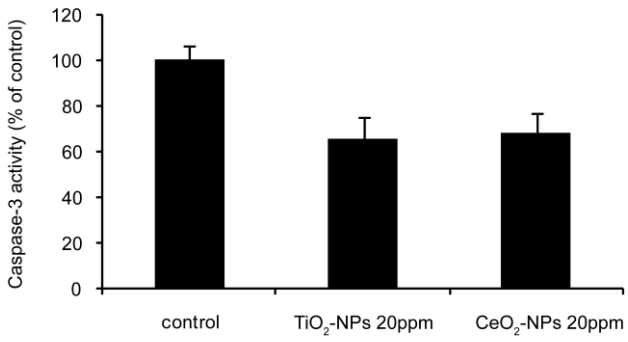

Figure S8: Caspase-3 activity. Cells were exposed to 20 ppm TiO_2-NPs and CeO_2-NPs. No increase of caspase-3 activity could be detected. Experiments were carried out in quintuplicates and repeated twice at the 24h time point. Values are mean ± SD.

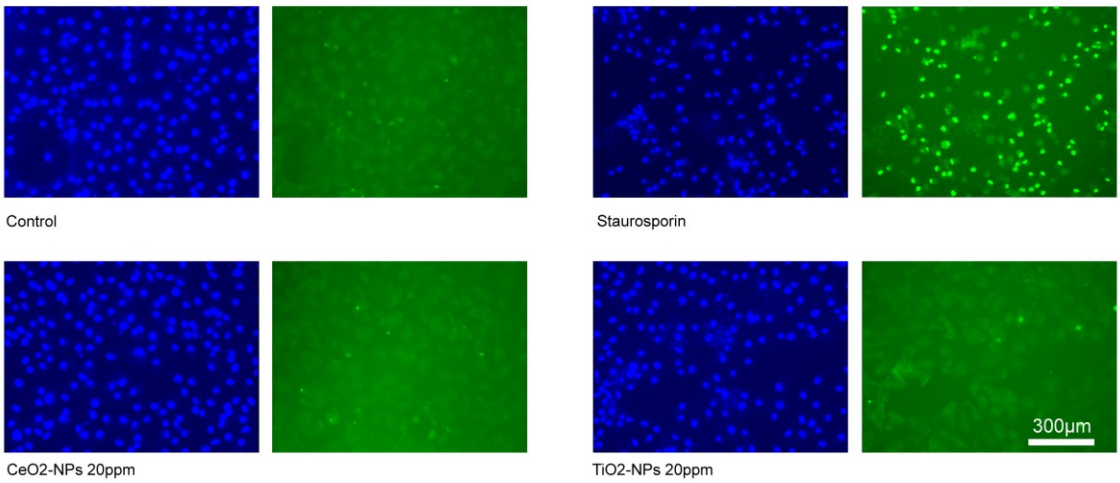

Figure S9: Immunofluorescence staining of apoptotic cells (green images) and the nuclear counterstain (blue images). Upon exposure to TiO_2-NPs and CeO_2-NPs for 24 hours no increase of TUNEL-positive cells could be detected.

References

Athanassiou, E.K., Grass, R.N., Stark, W.J., 2010. Chemical Aerosol Engineering as a Novel Tool for Material Science: From oxides to Salt and Metal Nanoparticles. Aerosol. Sci. Tech., 44(2), 161-72.

Brunner, T.J., Wick, P., Manser, P., Spohn, P., Grass, R.N., Limbach, L.K., Bruinink, A., Stark, W.J. 2006. In Vitro Cytotoxicity of Oxide Nanoparticles: Comparison to Asbestos, Silica, and the Effect of Particle Solubility. Environ Sci Technol. 40(14), 4374-81.

Limbach, L.K., Li, Y., Grass, R.N., Brunner, T.J., Hintermann, M.A., Muller, M., Gunther, D., Stark, W.J. 2005. Oxide Nanoparticle Uptake in Human Lung Fibroblasts: Effects of Particle Size, Agglomeration, and Diffusion at Low Concentrations. Environ Sci Technol. 39(23), 9370-6.

Limbach, L.K., Wick, P., Manser, P., Grass, R.N., Bruinink, A., Stark, W.J. 2007. Exposure of Engineered Nanoparticles to Human Lung Epithelial Cells: Influence of Chemical Composition and Catalytic Activity on Oxidative Stress. Environ Sci Technol. 41(11), 4158-63.

Loher, S., Stark, W.J., Maciejewski, M., Baiker, A., Pratsinis, S.E., Reichardt, D., Maspero, F., Krumeich, F., Gunther, D. 2005. Fluoro-apatite and Calcium Phosphate Nanoparticles by Flame Synthesis. Chem. Mater. 17 (1), 36–42.

Mädler,L., Kammler, H.K., Mueller, R., Pratsinis, S.E. 2002. Controlled synthesis of nanostructured particles by flame spray pyrolysis. J. Aerosol Sci. 33(2), 369-389.

Stark W.J. 2011. Nanoparticles in Biological Systems. Angew. Chem. Int. Ed. 50(6), 1242-58.

Vandeputte, C., Guizon, I., Genestie-Denis, I., Vannier, B., Lorenzon, G. 1994. A microtiter plate assay for total glutathione and glutathione disulfide contents in cultured/isolated cells: performance study of a new miniaturized protocol. Cell Biol Toxicol. 10(5-6), 415-21.